

Figure 1: *Left:* Example of objects included in the sample, the overlaid hexagonal fields correspond to the PPAK instrument FoV. *Right:* Radial oxygen abundance density distribution for the whole H II region spectroscopic sample. The first contour indicates the mean density, with a regular spacing of four times this value for each consecutive contour. The light-blue solid-circles indicate the mean value (plus $1 - \sigma$ errors) for each consecutive radial bin of $\sim 0.15 R_e$. The average error of the derived oxygen abundance is shown by a single error bar located at the top-right side of the panel. The solid-orange square indicates the average abundance of the solar neighbourhood, at the distance of the Sun to the Milky-Way galactic center.

The spatially-resolved information provided by these observations are allowing us to test and extend the previous body of results from small-sample studies, while at the same time open up a new frontier of studying the 2D oxygen abundance on discs and the intrinsic dispersion in metallicity, progressing from a one-dimensional study (radial abundance gradients) to a 2D understanding, allowing us at the same time to strengthen the diagnostic methods that are used to measure H II region abundances in galaxies. Here we present two highlights of our current studies employing this large spectroscopic database: 1) An IFS, statistical approach to the abundance gradients of spiral galaxies; and 2) The discovery of a new scaling relation of H II regions in spiral galaxies and how we use it to reproduce –with **remarkable** agreement– the mass-metallicity relation of star-forming galaxies.

2 Data sample and analysis

The studies here described were performed using IFS data of a sample of nearby disc galaxies (left-panel of Fig. 1), part belonging to the PINGS survey [7], and a sample of face-on spiral galaxies from [5], as part of the feasibility studies for the CALIFA survey [12]. The observations were designed to obtain continuous coverage spectra of the whole surface of the galaxies. The final sample comprises 38 objects, with a redshift range between ~ 0.001 - 0.025 . They were observed with the PMAS spectrograph [9] in the PPAK mode [15, 2] on the 3.5m telescope in Calar Alto with similar setup, resolutions and integration times, covering their optical extension up to ~ 2.4 effective radii within a wavelength range ~ 3700 - 7000 \AA . Details

on the sample, observing strategy, setups, and data reduction can be found in [7], and [5].

The H II regions in these galaxies were detected, spatially segregated, and spectrally extracted using HIIEXPLORER [13]. We detected a total of 2573 H II regions with good spectroscopic quality. This is by far the *largest* spatially-resolved, nearby spectroscopic H II region survey ever accomplished. The emission lines were decoupled from the underlying stellar population using FIT3D [10], following a robust and well-tested methodology [7, 11]. Extinction-corrected, flux intensities of the stronger emission lines were obtained and used to select only star-forming regions based on typical BPT diagnostic diagrams. The final sample comprises 1896 high-quality, spatially-resolved H II regions/aggregations of disc galaxies in the local Universe. Details on the procedure can be found in [13].

3 An IFS approach to abundance gradients

We used our catalogue H II regions to characterize the radial gradients of the gas-phase physical properties of the galaxy sample. The radial distance was normalised to the effective radius of each galaxy. The right-panel of Fig. 1 shows the radial density distribution for the oxygen abundance derived using the O3N2 indicator [6], once scaled to the average value at the effective radius for each galaxy. The solid line shows the average linear regression found for each individual galaxy. The red dashed line shows the actual regression found for all the H II regions detected for all the galaxies.

As discussed in [13], our results seem to indicate that there is an *universal* radial gradient for oxygen abundance when normalized with the *effective radii* of the galaxies. For each galaxy we derived the correlation coefficient, the slope and zero-point of a linear regression. A histogram of the slopes of the gradients are consistent with a Gaussian distribution, i.e. the dispersion of values found for each individual galaxy is compatible with the average one, not showing strong statistical deviations. A similar behaviour was found with the radial distribution of the equivalent width of H α .

4 The local \mathcal{M} -Z relation

The existence of a strong correlation between stellar mass and gas-phase metallicity in galaxies is a well known fact. The mass-metallicity (\mathcal{M} -Z) relation is consistent with more massive galaxies being more metal-enriched, it was established observationally by [14]. However, there has been no major effort to test the \mathcal{M} -Z relation using *spatially-resolved* information. We used our IFS observations in order to test the distribution of mass and metals *within* the discs of the galaxies. We derived the (luminosity) surface mass density (Σ_{Lum} , $M_{\odot} \text{ pc}^{-2}$) within the area encompassed by our IFS-segmented H II regions, using the prescriptions given by [1] to convert $B - V$ colors into a B -band mass-to-light ratio (M/L).

The left-panel of Fig. 2 shows the striking correlation between the local surface mass density and gas metallicity for our sample of nearby H II regions, i.e. the *local* \mathcal{M} -Z relation, extending over ~ 3 orders of magnitude in Σ_{Lum} and a factor ~ 8 in metallicity [8]. The notable similarity with the global \mathcal{M} -Z relation can be visually recognised with the aid of the

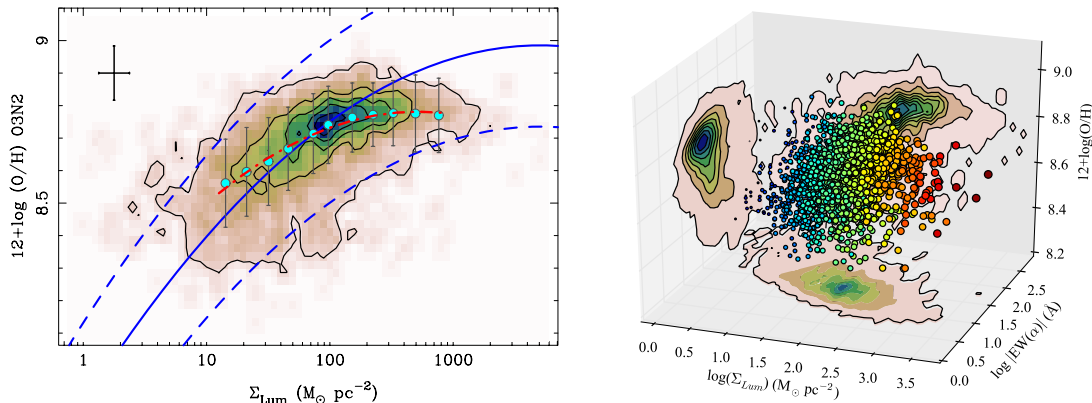


Figure 2: *Left-panel:* The relation between surface mass density and gas-phase oxygen metallicity for ~ 2000 H II regions in nearby galaxies, the *local* \mathcal{M} -Z relation. The first contour stands for the mean density value, with a regular spacing of four times this value for each consecutive contour. The blue circles represent the mean (plus 1σ error bars) in bins of 0.15 dex. The red dashed-dotted line is a polynomial fit to the data. The blue-lines correspond to the [14] relation (± 0.2 dex) scaled to the relevant units. Typical errors for Σ_{Lum} and metallicity are represented. *Right-panel:* 3D representation of the local \mathcal{M} -Z-EW(H α) relation. The size and color scaling of the data points are linked to the value of $\log \Sigma_{\text{Lum}}$ (i.e. low-blue to high-red values). The projection of the data over any pair of axes reduces to the local \mathcal{M} -Z, \mathcal{M} -EW(H α), and metallicity-EW(H α) relations. An online 3D animated version is available at: <http://tinyurl.com/local-MZ-relation>

blue-lines which stand for the [14] fit (± 0.2 dex) to the global \mathcal{M} -Z relation, shifted arbitrarily both in mass and metallicity to coincide with the peak of the H II region \mathcal{M} -Z distribution. Other abundance calibrations were tested obtaining the same shape (and similar fit) of the relation.

In addition, we find the existence of a more general relation between mass surface density, metallicity, and the equivalent width of H α , defined as the emission-line luminosity normalized to the adjacent continuum flux, i.e. a measure of the SFR per unit luminosity [3]. This functional relation is evident in a 3D space with orthogonal coordinate axes defined by these parameters, consistent with $|\text{EW}(\text{H}\alpha)|$ being inversely proportional to both Σ_{Lum} and metallicity, as shown in Fig. 2. As discussed in [8], we interpret the local \mathcal{M} -Z-EW(H α) relation as the combination of: i) the well-known relationships between both the mass and metallicity with respect to the differential distributions of these parameters found in typical disc galaxies, i.e. the *inside-out* growth; and ii) the fact that more massive regions form stars faster (i.e. at higher SFRs), thus earlier in cosmological times, which can be considered a local *downsizing* effect, similar to the one observed in individual galaxies.

In order to test whether the global \mathcal{M} -Z relation observed by [14] using SDSS data is a reflection (aperture effect) of the local H II region mass-density vs. metallicity relation, we perform the following exercise. We simulate a galaxy with typical M_B and $B - V$ values drawn from flat distributions in magnitude (-15 to -23) and colour (~ 0.4 – 1). A redshift is assumed for the mock galaxy, drawn from a Gaussian distribution with mean ~ 0.1 and $\sigma = 0.05$, with a redshift cut $0.02 < z < 0.3$ in order to resemble the SDSS [14] distribution.

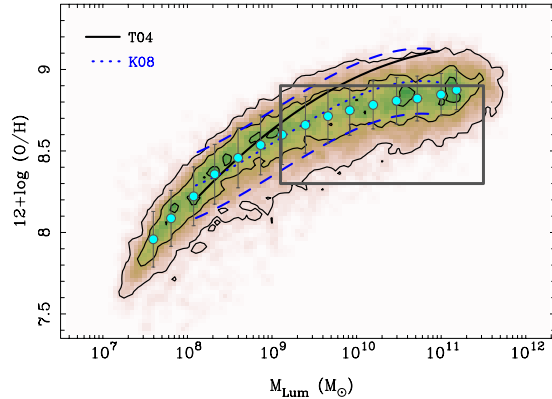


Figure 3: Distribution of simulated galaxies in the \mathcal{M} -Z plane assuming a *local* \mathcal{M} -Z relation and considering the aperture effect of the SDSS fiber, as explained in the text. The contours correspond to the density of points, while the circles represent the mean value (plus 1σ error bars) in bins of 0.15 dex. The black line stands for the [14] fitting, while the blue-lines correspond to the [4] ± 0.2 dex relation. The rectangle encompasses the range in mass and metallicity of the galaxy sample.

The mass of the galaxy is derived using the integrated B -band magnitudes, $B - V$ colours and the average M/L ratio following [1]. The metallicity of the mock galaxy is derived using the local \mathcal{M} -Z relation within an aperture equal to the SDSS fiber (3 arcsec), i.e. the metallicity that corresponds to the mass density surface at this radius. The process is repeated over 10,000 times in order to obtain a reliable distribution in the mass and metallicity of the mock galaxies.

Fig. 3 shows the result of the simulation, i.e. the distribution of the mock galaxies in the \mathcal{M} -Z parameter space. We reproduce –with a *remarkable* agreement– the overall shape of the global \mathcal{M} -Z relation assuming a local \mathcal{M} -Z relation and considering the aperture effect of the SDSS fiber. The overlaid lines correspond to the [14] fit (black) and the [4] ± 0.2 dex relation (blue), for which the agreement is extremely good over a wide range of masses. The result is remarkable considering that we are able to reproduce the global \mathcal{M} -Z relation over a huge dynamical range, using a local \mathcal{M} -Z relation derived from a galaxy sample with a restricted range in mass ($9.2 < \log M_{\text{Lum}} < 11.2$) and metallicity ($8.3 < 12 + \log(\text{O}/\text{H}) < 8.9$), indicated by the rectangle shown in Fig. 3.

5 Conclusions

By using ~ 2000 spatially-resolved H II regions of a sample of nearby galaxies observed with IFS, we found that the oxygen abundance presents a radial gradient that, statistically, has the same slope for all the galaxies when normalized to the effective radius, being independent of the morphology, suggesting an *universal* radial gradient for oxygen abundance [13]. The same effect is also seen with the equivalent width of H α . If true, this result put strong constraints to the structure of spiral galaxies.

We also demonstrate the existence of a *local* relation between the surface mass density, gas-phase oxygen abundance and $|\text{EW}(\text{H}\alpha)|$. The projection of this distribution in the metallicity vs. Σ_{Lum} plane is the *local* \mathcal{M} -Z relation, which notably has the same shape as the global \mathcal{M} -Z relation for galaxies. We use the local \mathcal{M} -Z relation to reproduce –with an *outstanding* agreement– the global \mathcal{M} -Z relation by means of a simple simulation which considers the aperture effects of the SDSS fiber at different redshifts. We conclude that, the \mathcal{M} -Z relation in galaxies is a scale-up integrated effect of a local \mathcal{M} -Z relation in the distribution of star-forming regions across the discs of galaxies [8].

Acknowledgments

Based on observations collected at the Centro Astronómico Hispano-Alemán (CAHA) at Calar Alto, operated jointly by the Max-Planck Institut für Astronomie and the Instituto de Astrofísica de Andalucía (CSIC). F.F.R.O. acknowledges the Mexican National Council for Science and Technology (CONACYT) for financial support under the programme Estancias Posdoctorales y Sabáticas al Extranjero para la Consolidación de Grupos de Investigación, 2010-2011 A.D. thanks the Spanish Plan Nacional de Astronomía programme AYA2010-21887 C04-03.

References

- [1] Bell, E. F., & de Jong, R. S., 2001, ApJ, 550, 212
- [2] Kelz, A., Verheijen, M. A. W., Roth, M. M., et al. 2006, PASP, 118, 129
- [3] Kennicutt, R. C. 1998, ARA&A, 36, 189
- [4] Kewley, L. J., & Ellison, S. L. 2008, ApJ, 681, 1183
- [5] Mármol-Queraltó, E., Sánchez, S. F., Marino, R. A., et al. 2011, A&A, 534, 8
- [6] Pettini, M., & Pagel, B. E. J. 2004, MNRAS, 348, L59
- [7] Rosales-Ortega, F. F., Kennicutt, R. C., Sánchez, S. F., et al. 2010, MNRAS, 405, 735
- [8] Rosales-Ortega, F. F., Sánchez, S. F., Iglesias-Páramo, J., et al. 2012, ApJ, 756, L31
- [9] Roth, M. M., Kelz, A., Fechner, T., et al. 2005, PASP, 117, 620
- [10] Sánchez, S. F., Cardiel, N., Verheijen, M. A. W., et al. 2007, MNRAS, 376, 125
- [11] Sánchez, S. F., Rosales-Ortega, F. F., Kennicutt, R. C., et al. 2011, MNRAS, 410, 313
- [12] Sánchez, S. F., Kennicutt, R. C., de Paz, A. G., et al. 2012, A&A, 538, 8
- [13] Sánchez, S. F., Rosales-Ortega, F. F., Marino, R. A., et al. 2012, A&A, in press (arXiv:1208.1117)
- [14] Tremonti, C. A., Heckman, T. M., Kauffmann, G., et al. 2004, ApJ, 613, 898
- [15] Verheijen, M. A. W., Bershady, M. A., Andersen, D. R., et al. 2004, AN, 325, 151